Surface circulation in the Alborán Sea (western Mediterranean) inferred from remotely sensed data

L. Renault,[1] T. Oguz,[1,2] A. Pascual,[3] G. Vizoso,[3] and J. Tintore[1,3]

Received 7 October 2011; revised 19 June 2012; accepted 20 June 2012; published 3 August 2012.

[1] In this study, for the first time at regional scale, the combined use of remote sensing data (altimetry and sea surface temperature records) provides a description of the persistent, recurrent and transient circulation regimes of the Alborán Sea circulation. The analysis of 936 altimeter-derived weekly absolute dynamic topography (ADT) and surface geostrophic current maps for 1993–2010 reveals the presence of a dominant annual signal and of two interannual modes of variability. The winter-spring phase is characterized by two stable gyral scale features; the well-known Western Anticyclonic Gyre within the western area and the Central Cyclonic Gyre, a new structure not identified in former studies, occupying the central and eastern parts of the Alborán Sea. A double anticyclonic gyre regime constitutes the stable circulation system of the summer–autumn period when the Eastern Anticyclonic Gyre is formed within the eastern Alborán basin. In this case, the Central Cyclonic Gyre is narrower and located closer to the Western Anticyclonic Gyre. They represent two stable states of the system, robust at the decadal time scale, whereas transient changes reflect perturbations on these stable states and are mainly observed at an interannual scale. The circulation variability and the gyral features development may be dynamically linked to the corresponding changes of the Gibraltar transport rates.

Citation: Renault, L., T. Oguz, A. Pascual, G. Vizoso, and J. Tintore (2012), Surface circulation in the Alborán Sea (western Mediterranean) inferred from remotely sensed data, *J. Geophys. Res.*, *117*, C08009, doi:10.1029/2011JC007659.

1. Introduction

[2] The ocean interacts with the atmosphere on multiple times-scales and the associated impacts on marine ecosystems are of worldwide attention. In particular, processes involved in the annual cycle, their dominant mode of variability may likely trigger variability on wide range of time scales (interannual to interdecadal) and can as well be modulated by longer time scale variability through feedback mechanisms. Coastal, semi-enclosed and marginal seas are a major concern since natural climatic variations are masked by those introduced through heavy human activities. The Alborán Sea in the western Mediterranean is a highly dynamic system known to exhibit complex set of interactions arising from local, regional and hemispherical processes, and therefore serves a good example for semi-enclosed seas [*Criado-Aldeanueva et al.*, 2012; *Vargas-Yáñez et al.*, 2010].

[3] Observations from field campaigns that have been conducted so far together with additional support from the AVHRR-Sea Surface Temperature (SST) imagery elucidated different synoptic views of the Alborán Sea circulation system. The Atlantic Jet (AJ) [e.g., *Tintoré et al.*, 1991; *Viúdez et al.*, 1998], that enters the Alborán Sea through the Strait of Gibraltar (Figure 1), is the main forcing of the hydrodynamic processes in Alborán. It flows with an estimated speed of about 1 m.s^{-1} [*García Lafuente et al.*, 2000] and drive the circulation in the Alborán Sea [*Parrilla and Kinder*, 1987; *Viúdez et al.*, 1996] influencing coastal upwelling in the northwestern sector of the basin [e.g., *Sarhan et al.*, 2000]. The AJ feeds the Western Anticyclonic Gyre (WAG) with an apparent year around persistence with a typical diameter of 100–150 km located roughly between the Gibraltar strait and 3.5°W longitude (Figure 1). A less intense and recurrent anticyclone called the Eastern Anticyclonic Gyre (EAG) may occasionally exist between 2.5°–1.5°W longitude and is also fed by the AJ (Figure 1). The WAG and EAG are roughly situated over the western and eastern Alborán basins having respective maximum depths of 1200 m and 1800 m and separated from each other by the Alborán Ridge (Figure 1). The Almeria-Oran front residing along eastern flank of the EAG [*Tintore et al.*, 1988; *Allen et al.*, 2001] forms the eastern limit of the Alborán circulation system. According to *Viúdez et al.* [1996, 1998], *Vargas-Yáñez et al.* [2002], *Macías et al.* [2008], the two gyres (WAG + EAG) circulation regime prevails in summer months and the single anticyclonic gyre (WAG) and/or coastal jet regime in winter months.

[4] Satellite altimetry has also provided some insights on the variability of the Alborán Gyres. Based on the analysis of 7 years (October 1992 to December 1999) of the TOPEX/

[1]SOCIB, Palma de Mallorca, Spain.
[2]Institute of Marine Sciences, METU, Mersin, Turkey.
[3]IMEDEA, UIB-CSIC, Esporles, Spain.

Corresponding author: L. Renault, SOCIB, Parc Bit, Naorte, Bloc A 2 p. pta. 3, Palma de Mallorca, ES-07121, Spain. (lrenault@imedea.uib-csic.es)

0148-0227/12/2011JC007659

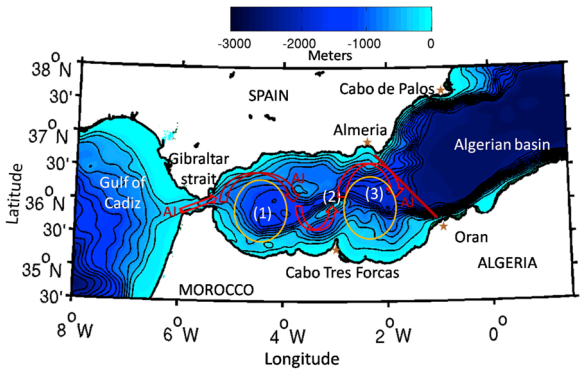

Figure 1. The studied region illustrated by the topography. Color fields and contours (one contour each 400 m) represent the bathymetry. The red line represents the approximate position of the Almeria-Oran front, and the star shows the key geographic locations indicated in the text. The red arrows represent the approximate boundary of the Atlantic Jet. And the orange circles display the Western Anticyclonic Gyre (WAG) and the Eastern Anticyclonic Gyre (EAG) positions, the numbers 1, 2, 3 in parentheses refer to the Western Alborán basin, the Alborán ridge, and the Eastern Alborán basin, respectively.

Poseidon (T/P) and ERS-1/2 sea level anomaly (SLA) data [*Larnicol et al.*, 2002], the western and eastern Alborán gyres are among the most intense and well-defined signals in the Mediterranean Sea and exhibit a clear seasonal cycle with an intensification in summer. The subsequent analysis of 11 years (1993–2003) merged (T/P, Jason, ERS and Envisat) altimetric data [*Pujol and Larnicol*, 2005] also showed maximum energy observed in late summer. Roughly half of the annual signal was attributed to the steric effect and the other part to the surface circulation with large spectrum of spatial and temporal scales. A very weak semiannual signal also existed with the RMS of SLA less than 3 cm.

[5] The main objective of this study is to document the temporal variability of the Alborán Sea circulation using 18 years of altimeter data and satellite Sea Surface Temperature (SST) data. In this sense, the present work is an extension of the studies by *Larnicol et al.* [2002] and *Pujol and Larnicol* [2005]. The main focus is the use of the absolute dynamic topography (ADT) obtained by adding a MDT [*Rio et al.*, 2007] to the SLA that allows overcoming some uncertainties in the study of the Alborán Sea circulation. On one hand: the lack of a MDT in the former altimetric studies does not allow concluding about the presence or disappearance of the Alborán gyres, but just its weakening or intensification. In this study, for the first time at regional scale, the use of ADT can provide a description of the persistent, recurrent and transient circulation regimes of the Alborán Sea circulation. On the other hand, ADT records are then compatible with satellite SST images that can be used as a complementary data set to describe the different Alborán Sea circulation states. Furthermore, our understanding of the primary modes of temporal and spatial variability in the Alborán Sea is far from complete, and deserves more extensive analysis. The present study attempts to improve our understanding of the Alborán Sea circulation, and to elaborate its circulation regimes using the satellite altimeter absolute dynamic topography and sea surface temperature data.

[6] The paper is structured as follows: section 2 introduces the data set. Section 3 provides a description of the persistent circulation as well as the recurrent and transient regimes. The results are then discussed in section 4, which is followed by the conclusions.

2. Data

[7] The weekly Absolute Dynamic Topography (ADT) fields are obtained from 18 years (1993–2010) of satellite altimeter data for the region bounded by 6°W to 1.5°E in longitude and 35°N to 38°N in latitude. They are based on the AVISO gridded products formed by merging all the available altimeter mission (Topex/Poseidon, Jason-1, Jason-2, ERS 1/2, ENVISAT) and available at http://www.aviso.oceanobs.com/duacs/. The data are based on a square grid of 0.125° (close to the Rossby internal radius of deformation of the region) constructed by optimal interpolation in time and space from combined and intercalibrated altimeter missions using objective analysis [*Le Traon et al.*, 1998]. The method to obtain gridded fields of merged Sea Level Anomalies (SLA) is described in *Pujol and Larnicol* [2005] and *Pascual et al.* [2007], with specific temporal and spatial correlation scales for the Mediterranean Sea. The weekly ADT maps are produced by adding the MDT data deduced from oceanic observations and an ocean general circulation model to the SLA fields [*Rio et al.*, 2007]. As documented by *Pujol and Larnicol* [2005], the resulting data set was able to document major observed circulation features and capable of monitoring short time (weekly to-monthly) variability mainly dominated by mesoscale structures in different regions of the Mediterranean Sea. It also identifies low frequency variability as a major part of the SLA signal. On the scale of the Alborán Sea, it is expected that the model-based MDT estimation may involve some error. However, it should not be critical to affect the spatial structures of annually stable circulation dynamics we study here as they are persistently observed in the entire 18 years data set and are identified by strong SLA signals. Note that the altimeter data coverage starts at 4.75°W longitude and thus does not capture the details of flow structure in the close vicinity of the Gibraltar strait.

[8] The surface geostrophic currents are computed by the weekly ADT fields, and used for interpretation of the circulation system using the geostrophic approximation by finite differences:

$$U_g = -\frac{g}{f}\frac{\partial \eta}{\partial y} \tag{1}$$

$$V_g = \frac{g}{f}\frac{\partial \eta}{\partial x} \tag{2}$$

with η as the ADT, g the gravity acceleration, f the Coriolis parameter and Ug and Vg the zonal and meridional geostrophic currents, respectively. Then, kinetic energy per unit of mass is computed as

$$KE = \frac{1}{2}\left(U_g^2 + V_g^2\right) \tag{3}$$

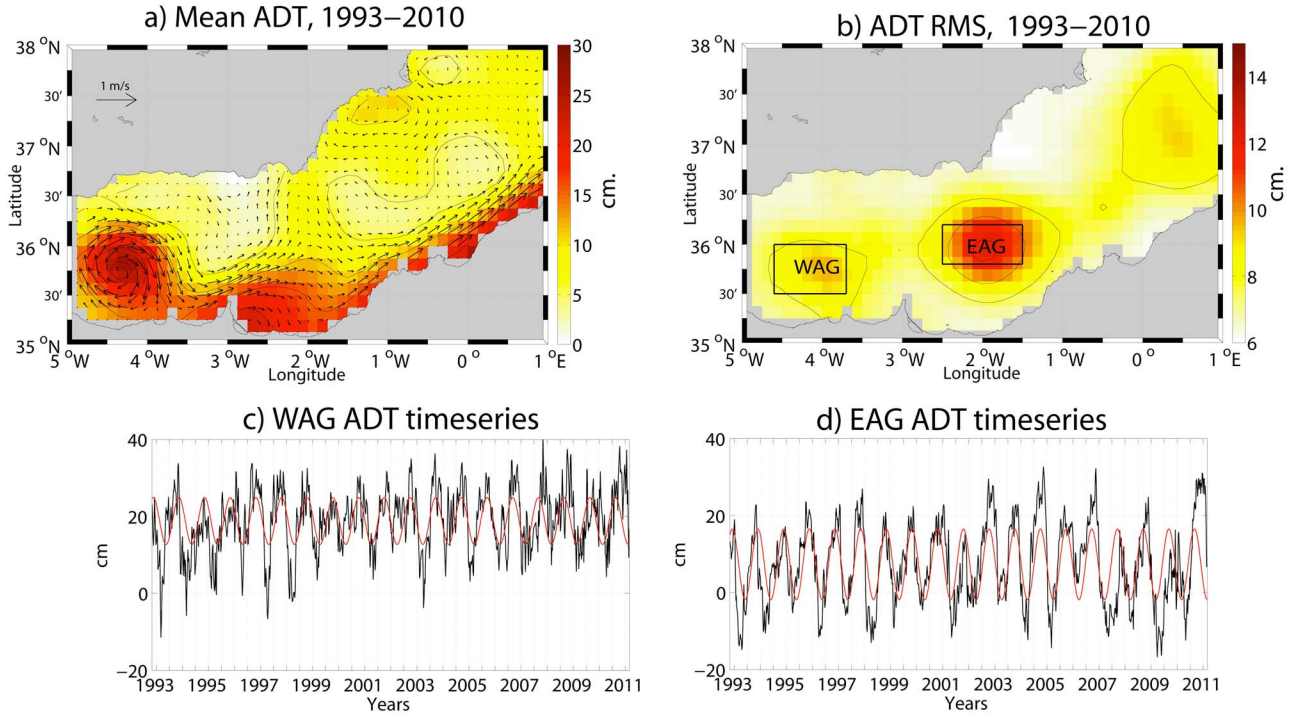

Figure 2. (a) Mean Absolute Dynamic Topography (ADT, in cm and in color) and associated geostrophic current direction and intensity (arrows) over the period 1993–2010. (b) RMS of the ADT over the same period (in cm). The black boxes represent the areas used to compute spatial averaged time series of the Western Anticyclonic Gyre (WAG) and the Eastern Anticyclonic Gyre (EAG), which are indicated by their acronyms. (c) Temporal variation of the averaged ADT (black) and the associated annual harmonic (red) over the WAG area indicated in Figure 2b. (d) Same as Figure 2c but for the EAG.

[9] The complementary SST data are provided by high resolution (~5 km) daily time series of the infrared AVHRR data for the Mediterranean basin [*Marullo et al.*, 2007]. This data set is compatible with in situ measurements with a mean bias less than 0.1°C and RMS error of about 0.5°C.

3. Results

3.1. Mean Circulation and RMS

[10] The mean circulation of the Alborán Sea can be described from Figure 2a that presents the mean ADT and geostrophic currents averaged over the period 1993–2010. Note, the mean ADT is similar to the MDT from *Rio et al.* [2007] suggesting that the 1993–2010 and the 1993–1999 mean are very similar. Consistent with former studies [e.g., *Viúdez et al.*, 1996, 1998], the mean circulation of the Alborán Sea is characterized by the presence of the AJ, characterized by mean currents up to of 0.5 $m.s^{-1}$ and by the WAG located roughly between the Gibraltar strait and 3.5°W longitude with a typical diameter of 100–150 km. As illustrated by the Root Mean Square (RMS) of the ADT (Figure 2b), the WAG appears to be a robust and persistent feature since ADT mean is much larger than its variability. The presence of the EAG can be identified by the less intense ADT between 2.5°–1.5°W longitude. The RMS of the ADT confirms the temporal characteristic of the EAG by a larger ADT variability than the mean. A closer focus on the ADT time series of the WAG and EAG obtained for the rectangular boxes of [4.6°W–3.7°W; 35.5°N–36°N] and [2.5°W–1.5W; 35.8°N–36.2°N], respectively, indicates a clear seasonal cycle of both gyres, which is marked by an ADT maximum in summer and minimum in winter (Figures 2c and 2d). As a matter of fact, it confirms the year-round persistence of the WAG and show the EAG is generally well defined during the summer and collapses during the winter. The characteristics of the two circulation regimes are assessed below.

3.2. EOF Analysis and Spatiotemporal Characteristics

[11] We applied an Empirical Orthogonal Function (EOF) analysis to the 936 weekly ADT data after removing the mean state (ADT mean). The obtained modes have to be interpreted as the variation of the circulation with respect to the mean state (see Figure 2a). The analysis reveals that the first EOF mode explains nearly 60% of the variance. As in *Cazenave et al.* [2002], it depicts the steric contribution of the seasonal signal and leads to an intensification or a weakening of both WAG and EAG (Figure 3a) respectively during the spring-summer and the winter-fall since the associated time series attains its maximum in late summer–early autumn (September–November, Figure 4a) and minimum in late winter–early spring (February–April) that can induce to the formation of the Central Cyclonic Gyre (CCG). The latter is pointed out for the first time as a stable feature of the surface circulation system in the present analysis. The second and third modes are weaker and constitute respectively 15% and 10% of the variance. The spatial pattern of the second mode reveals a marked dipole between the EAG and the cyclonic eddy east of the EAG, with a well-defined Almería-Orán

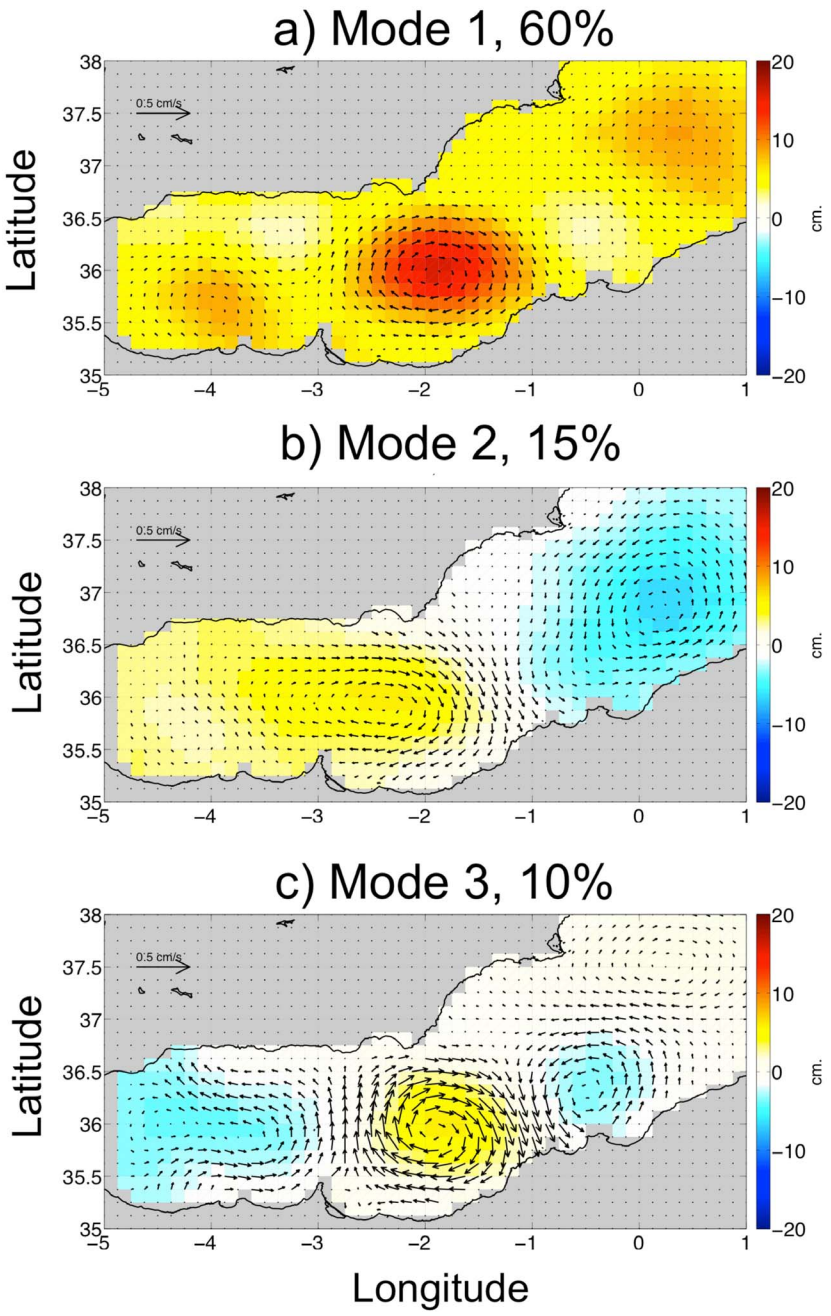

Figure 3. The three first Empirical Orthogonal Function (EOF) modes applied on the ADT fields after removing the mean overall the period. The colors represent the spatial variations of the (a) first EOF mode (explained variance of 60% of the total variance), (b) second EOF mode (explained variance of 15% of the total variance), and (c) third EOF mode. The associated geostrophic circulation is indicated by the arrows (in cm/s).

front (Figures 3b and 3c). It represents the intensification and weakening of the EAG at interannual timescale (Figures 4b and 4c). The spatial pattern of the third mode represents, in opposite phase, an intensification (weakening) of WAG and a weakening (intensification) of the EAG as well as the presence of an anticyclonic (cyclonic) eddy east of the EAG. A spectral analysis of these modes reveals the dominant frequencies are 2–2.5 years (Figures 4b and 4c). Additionally, a frequency of 5 years also appears significant (at 95% using a Markov red noise [e.g., *Cusick and Flahive*, 1989]) in the second mode, however, the time series is too short to determinate clearly such variability. Finally, the fourth mode represents only 7.2% of the variance and leads to some intensification and weakening of the WAG and EAG at intraseasonal timescale (not shown). These interannual and intraseasonal modes, as explained bellow, explain some transient mode of the Alborán Sea circulation.

[12] A closer focus on the kinetic energy (KE) time series of the WAG and EAG obtained for the rectangular boxes of [4.6°W–3.7°W; 35.5°N–36°N] and [2.5°W–1.5°W; 35.8°N–

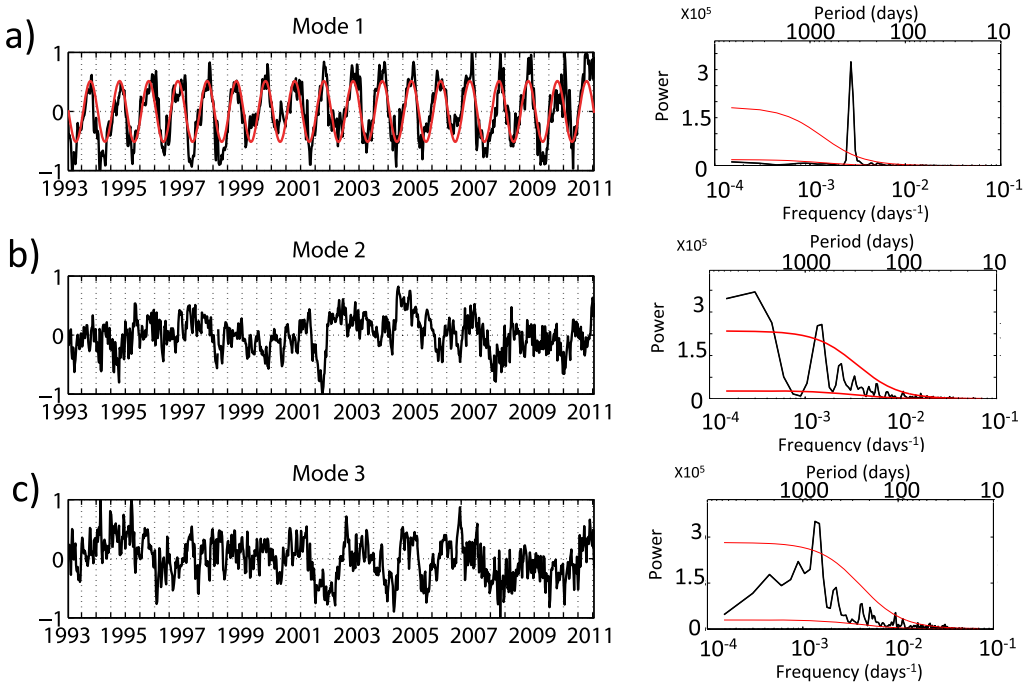

Figure 4. On the left, the black and red line represent respectively the full signal and annual harmonic of the temporal variations of the (a) first Empirical Orthogonal Function mode, (b) second EOF mode and (c) third EOF mode of the Sea Level Anomalies (estimated by removing the 1993–2010 ADT mean from the ADT fields) data for the Alborán Sea. On the right are the spectra of the associated time series; the upper (lower) scale provides the period (frequency). The red lines represent the 5% and 95% confidence interval estimated from a red noise (Markov).

36.2°N], respectively, further shows that the energy of WAG is in general three times higher than that of the EAG (Figures 5a and 5b) for the whole year due to its interaction with the stronger AJ [*Viúdez et al.*, 1998] immediately after issuing from the Gibraltar strait. Both gyres acquire relatively strong KE during the second half of the years and vice versa for the first half. The KE of the EAG declines close to zero during winter indicating its disappearance (Figures 5b and 5c), whereas the WAG is able to preserve its existence although its energy decreases substantially for some weeks (Figures 5a and 5c). These findings suggest the first EOF mode combined with the mean state may be interpreted by the year-around persistence of the WAG but the presence of the EAG only during the second half of the year and its replacement by the CCG during the first half.

[13] Table 1 documents the monthly classification of likely circulation regimes as inferred visually by the weekly ADT fields for the entire data set (1993–2010). The distinguishing feature is composition of the annual signal by the single and double anticyclonic circulation regimes (referred by 1G and 2G in Table 1, respectively) with a distinct seasonal character. A triple anticyclonic gyre system (WAG, CAG, EAG, denoted 3G in Table 1) emerges only occasionally in the form of short-term transients (Figure 6) and can be explained by the intraseasonal fourth EOF mode (not shown). Another transient regime is a two gyres system with the center of EAG shifted eastward to 0.5°W longitude (2GD). The use of the EOFs modes reveals this transient regime is induced by the third EOF mode (Figures 3c and 4c). Finally, a Coastal Jet mode (CJ) appears also as a short-term transient but is not captured by the EOF analysis meaning it is not statistically significant (Figure 6). In 14 out of 18 years, the winter–spring phase is characterized by the WAG only (the single anticyclonic gyre system) contrary to an additional development of the EAG and thus the double gyres system during the summer–autumn period. The alternation between these two regimes appears to take place only within few weeks. Another way of interpretation of these two annual regimes is the persistence of WAG for the entire year and the presence of the EAG over the latter half of the year and displacement of the CCG location accordingly. We recall that these regimes are depicted by an almost twofold to threefold increase in the kinetic energy storage of WAG and EAG from winter to summer period (Figures 5a and 5b). This stable regime can be interpreted as the first EOF mode as revealed by the EOF analysis. Some years, however, are dominated entirely by the single anticyclonic gyre (e.g., 2007, 2009) or the double gyres (e.g., 1995, 2006) circulation system. A reconstruction of the signal using the EOFs modes allows linking these anomalies to the second and third EOFs modes (not shown) that lead to a reinforcement or a weakening of the WAG/EAG at interannual timescale (Figures 3 and 4). Further details of the emerging circulation systems are described below.

3.3. Persistent Circulation Regimes

[14] The long-term (1993–2010) mean patterns of the single and double gyre anticyclonic circulation systems are displayed in Figures 7a and 7b, respectively, as the average maps of all the circulation patterns that are designated by 1G and 2G in Table 1. In the case of single anticyclonic gyre

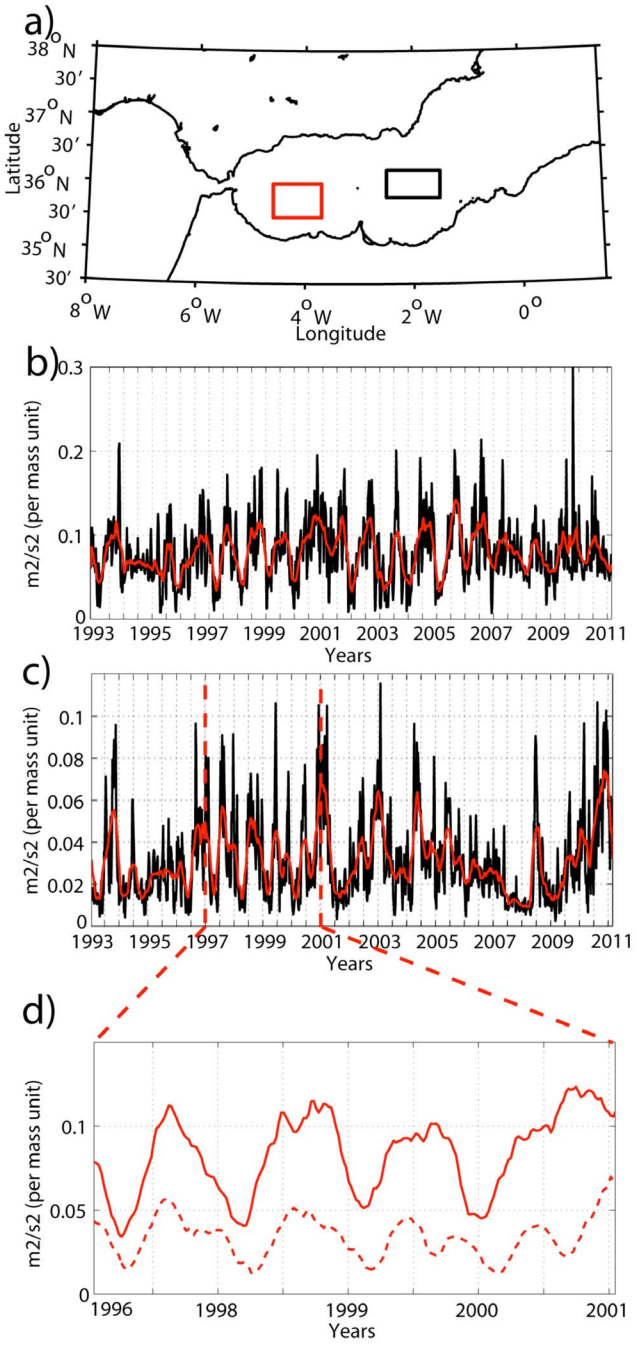

Figure 5. (a) Boxes defined to estimate the time series for the Western Anticyclonic Gyre (WAG, red box) and Eastern Anticyclonic Gyre (EAG, black box). (b) Time series of total kinetic energy ($m2s^{-2}$ per mass unit) for the WAG box during 1993–2010. (c) Same as Figure 5b for the EAG box. (d) Zoom over the 1997–2001 period, the red continuous and dashed lines are respectively the WAG and EAG filtered data.

system (Figure 7a), the region comprises the WAG and the Central Cyclonic Gyre (CCG) situated over the western and eastern Alborán basins, respectively. The northwestern coastal zone is associated with relatively colder waters (SST ∼ 16.8–17.0°C) with respect to rest of the basin (∼17.4–17.8°C). A cold patch in this region may likely develop in response to frequent wind-induced coastal upwelling events that prevail during the winter and spring seasons in the region [e.g., *Macías et al.*, 2008]. The periphery of the WAG and the coastal jet along the south coast are characterized by surface currents of 0.3–0.5 m s^{-1} and relatively warmer mean SST with respect to its surrounding waters. The highest kinetic energy is maintained within the region of the WAG with magnitudes less than 0.1 m^2 s^{-2}. The magnitude of currents within the interior of CCG is about 0.2 m s^{-1} and they typically acquire weak kinetic energy, less than 0.02 m^2 s^{-2}.

[15] The double gyre circulation system (Figure 7b) may be considered as a slightly modified version of the single anticyclonic gyre circulation, in which the CCG becomes narrower and is located closer to the WAG and its former position is occupied by the EAG that is roughly centered at 2°W longitude. A distinguishing feature of the double gyre circulation system is the presence of relatively cold water mass (characterized by SST ∼ 19.5–20.5°C) within the western part of the basin up to the EAG (Figure 7b). The cold water mass is evidently of the Atlantic origin, and indirectly infers to the case of stronger Atlantic inflow that is also marked by stronger geostrophic currents and kinetic energies (∼0.13 m^2 s^{-2} within the WAG) with respect to the single anticyclonic gyre system. The Almeria-Oran frontal zone separates this relatively cold surface layer water mass structure from the warmer (SST ∼ 21.5–22.0°C) modified Mediterranean water mass of the Algerian basin. The Eastern Cyclonic Gyre (ECG) in the western Algerian basin and an anticyclonic eddy located its further north between Almeria and Cabo de Palos (see Figure 1) are other quasi-persistent

Table 1. The Monthly Classification of Different Circulation Regimes During 1993–2010 as Inferred by Weekly Average Absolute Dynamic Topography (ADT) Fields[a]

	Month											
Year	1	2	3	4	5	6	7	8	9	10	11	12
1993	**1G**	**1G**	**1G**	**1G**	**1G**	*2G*	*2G*	*2G*	*2G*	*2G*	*2G*	***1G***
1994	**1G**	**1G**	**1G**	**1G**	*2G*	*2G*	*2G*	*2G*	*2G*	*2G*	*2G*	*2G*
1995	*2G*	*2G*	*2G*	*2G*	*2G*	*2G*	*2G*	*2G*	*2G*	*2G*	*3G*[b]	*2G*
1996	*2G*	**1G**	**1G**	**1G**	**1G**	**1G**	*2G*	*2G*	*2G*	*2G*	*2G*	*2G*
1997	**1G**	**1G**	**1G**	**1G**	**1G**	**2G**	*2G*	*2G*	*2G*	*2G*	*2G*	**1G**
1998	**1G**	CJ[b]	**1G**	**1G**	**1G**	**1G**	**1G**	*2G*	*2G*	*2G*	**1G**	**1G**
1999	**1G**	**1G**	**1G**	*2G*	*2G*	*2G*	*2G*	*2G*	*2G*	*2G*	**1G**	**1G**
2000	**1G**	**1G**	*2G*	*2G*	*2G*	*2G*	*2G*	*2G*	*2G*	*2G*	*2G*	*2G*
2001	*2G*	*2G*	**1G**	**1G**	*2G*	*2GD*[b]	*2GD*[b]	*2GD*[b]	*2GD*[b]	*2GD*[b]	**1G**	**1G**
2002	**1G**	**1G**	**1G**	**1G**	**1G**	*2G*	*2G*	*2G*	*2G*	*2G*	*2G*	*2G*
2003	*2G*	**1G**	**1G**	**1G**	**1G**	*2G*	*2G*	*2G*	*2G*	*2G*	*2G*	*2G*
2004	**1G**	*2GD*[b]	**1G**	**1G**	*2G*	*2G*	*2G*	*2G*	*2G*	*2G*	*2G*	**1G**
2005	**1G**	**1G**	**1G**	**1G**	*2G*	*2G*	*2G*	*2G*	*2G*	*2G*	*2G*	*2G*
2006	*2G*	*2G*	*2G*	*2G*	*2G*	*2G*	*2G*	*2G*	*2G*	*2G*	*2G*	*2G*
2007	*2G*	**1G**	**1G**	**1G**	**1G**	**1G**	**1G**	**1G**	**1G**	**1G**	**1G**	**1G**
2008	**1G**	**1G**	**1G**	**1G**	**1G**	**1G**	**1G**	*2G*	*2G*	*2G*	*2G*	**1G**
2009	**1G**	**1G**	**1G**	**1G**	**1G**	**1G**	**1G**	**1G**	**1G**	**1G**	**1G**	**1G**
2010	**1G**	**1G**	**1G**	**1G**	**1G**	*2G*	*2G*	*2G*	*2G*	*2G*	*2G*	**1G**

[a]Here 1G refers to the presence of Western Anticyclonic Gyre (WAG) only; 2G refers to the presence of both WAG and Eastern Anticyclonic Gyre (EAG); 3G refers to the presence of triple anticyclonic gyres: WAG, Central Anticyclonic Gyre (CAG) and EAG; 2GD refers to the two gyres system with the center of EAG shifted eastward to 0.5°W longitude; CJ is the coastal jet mode. The 1G and 2G modes are the quasi-permanent features. Distinct seasonal characters of the 1G and 2G regimes are marked by bold and italics.

[b]Recurrent/transient modes of the circulation.

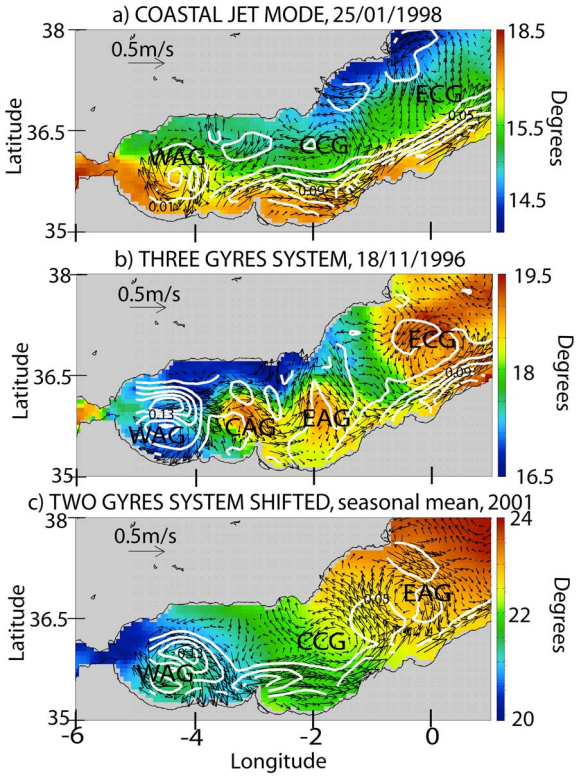

Figure 6. Same as Figure 5 but for recurrent/temporal modes of the Alborán Sea gyral circulation system. They correspond to (a) coastal jet (transient, CJ) mode with low rate of Atlantic inflow, (b) three-gyre (transient, 3G) mode with higher rate of Atlantic inflow in which CAG develops between WAG and EAG, and (c) two-gyres (recurrent, 2GD) mode with higher rate of Atlantic inflow in which EAG is displaced toward east. The color bars on the right represent the SST ranges in °C. The respective positions of the Western Anticyclonic Gyre (WAG), Central Cyclonic Gyre (CCG), Eastern Anticyclonic Gyre (EAG) and Eastern Cyclonic Gyre (ECG) are indicated by the respective acronyms.

features. But they are not formally members of the Alborán Sea circulation system.

3.4. Recurrent and Transient Circulation Regimes

[16] A notable temporal modification relates to degradation of the single anticyclonic gyre circulation mode into the coastal jet mode. According to *Vargas-Yáñez et al.* [2002], the loss of the WAG is favored when the parameter $u(fR_w)^{-1}$ reduces below unity at the Gibraltar exit; in this case the Coriolis force holds the jet attached to the southern coast. Taking the radius of curvature at the southeast exit corner near Ceuta as $R_w \approx 5$ km [*Bormans and Garrett*, 1989] and the Coriolis parameter $f = 10^{-4}$ sec^{-1}, this condition holds for a typical surface current magnitude of $u < 0.5$ ms^{-1}. An example of this event has been formerly presented by *Vargas-Yáñez et al.* [2002] for January–February 1998. It prevailed until the single anticyclonic gyre circulation mode developed by the second half of March 1998. It has been triggered by strong easterlies associated with changes in the surface atmospheric pressure field that has led subsequently to an abrupt drop of the upper layer transport from 1.3 Sv to 0.3 Sv and a corresponding increase in the lower layer transport from 0.8 Sv to 1.1 Sv, and thus a reversal of the net transport toward the Gulf of Cadiz [*García-Lafuente et al.*, 2002]. Weakening of the upper layer transport may have several consequences: (1) it weakens anticyclonic vorticity of the Atlantic inflow through the Gibraltar strait that then permits the Atlantic Jet to deflect more preferentially toward the south coast under the effect of the Coriolis force, (2) it diminishes the momentum support for maintain the WAG and thus causes its gradual dissipation. Thus, the circulation system may be left by only a coastal jet and a set of weak eddies that are dispersed within the basin.

[17] The surface circulation map derived from the altimeter data for the week that is centered at 25 January 1998 (Figure 6a) and the subsequent maps, however, do not show the loss of the WAG as asserted by *Vargas-Yáñez et al.* [2002]. Instead, the WAG is able to preserve its identity with much weaker kinetic energy availability (less than 0.05

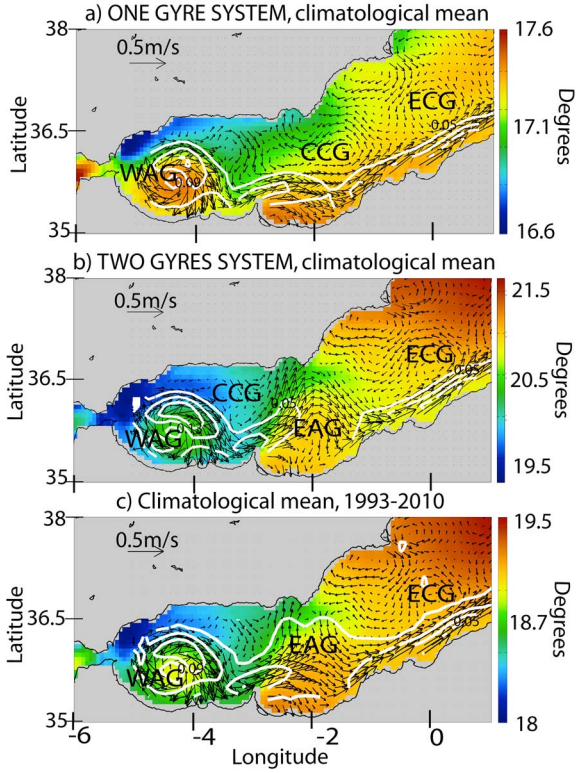

Figure 7. Geostrophic current (m s^{-1}) patterns and kinetic energy (m^2 s^{-2}, one contour each 0.05 m^2 s^{-2}) distributions superimposed on the weekly mean SST fields for the two quasi-persistent modes of the Alborán Sea gyral circulation system. They correspond to (a) one-gyre mode (1G) with moderate rate of Atlantic inflow, (b) two-gyres mode (2G) with high rate of Atlantic inflow, and (c) mean over the 1993–2010 period. The 1G and 2G circulation maps represent the mean of the all available similar cases. The color bars on the right represent the SST ranges in °C. The respective positions of the Western Anticyclonic Gyre (WAG), Central Cyclonic Gyre (CCG), Eastern Anticyclonic Gyre (EAG) and Eastern Cyclonic Gyre (ECG) are indicated by the respective acronyms.

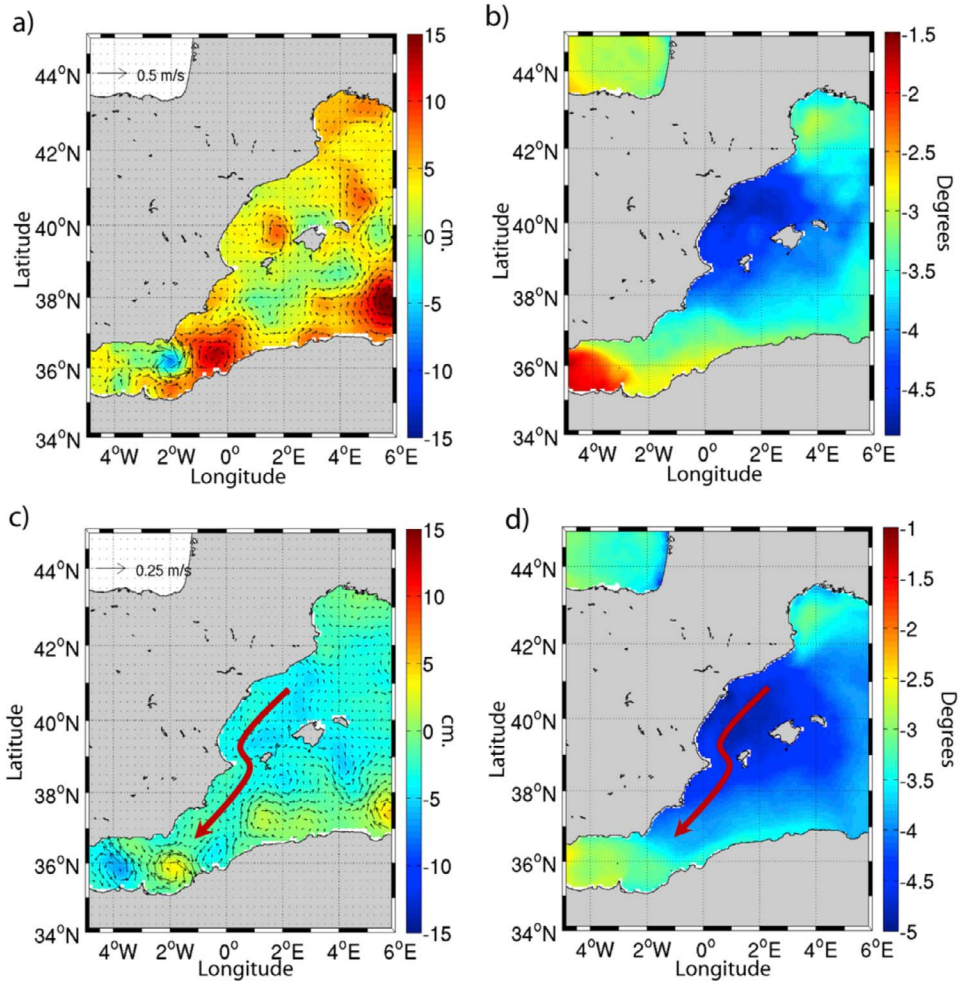

Figure 8. (a) The color fields (arrows) represent the differences in cm (in m/s) between the mean Absolute Dynamic Topography (mean geostrophic currents) during winter 2009–2010 (01/12/2009–01/03/2010) and the mean Absolute Dynamic Topography (mean geostrophic current) over the 1993–2010 period. For clarity, vectors are shown every 2 grids points. (b) Same as Figure 8a but for the Sea Surface Temperature. (c) Same as Figure 8a but for the differences between the period the anomalous winter (1995, 2001 and 2006) and the 1993–2010 period. (d) Same as Figure 8c but for the Sea Surface Temperature. The red arrows highlight the southward current that advects colder Mediterranean water.

$m^2\ s^{-2}$). Because of the lack of data coverage at immediate vicinity of the Gibraltar strait, the altimeter data cannot resolve precisely whether the WAG shown in Figure 6a is fed, albeit weakly, by the inflow or is decoupled completely from the inflow and is in the process of gradual dissipation. In any case, the north-south temperature gradient associated with a warmer SST structure of the Gibraltar Strait and along the southern coast (17–18.0°C) with respect to the colder northern part (15.0–15.5°C) may support preferential deflection of the inflow toward the south coast. As in the case of altimeter data, this SST contrast however may not completely rule out a possibility of partial feeding of the WAG by the inflow, or preserving its identity for few months even in the case of decoupling.

[18] Another transient mode of the circulation system is the transformation of the double gyre circulation system to a triple gyre system (Figure 6b) for which various case studies have been documented by *Viúdez et al.* [1998], *Vargas-Yáñez et al.* [2002], *Vélez-Belchí et al.* [2005], *Flexas et al.* [2006] during autumn 1996, 1997, 2003. This system typically prevails at a time scale of one month after which it reverts back to a standard double gyre system. An example for mid-November 1996 is displayed in Figure 6b. Slightly higher geostrophic current and kinetic energy estimates of this regime with respect to the double gyre mode infer that its occurrence requires relatively high Atlantic inflow rate with respect to that of the standard double gyre case. Note a reconstruction of the signal using the EOFs modes allows to link this transient regime to the fourth EOF mode (not shown).

[19] Another modification of the double gyre system, which is encountered only once during June–October 2001 within the entire data set, is the eastward shift of the EAG beyond the Almeria-Oran cross-section (Figure 6c). It effectively replaces the ECG centered roughly at 0.5°W longitude. The broad region between the WAG and EAG is then occupied by the CCG as in the case of one-gyre system.

Thus, as far as the Alborán Sea circulation is concerned, this case corresponds to a variant of the single anticyclonic gyre regime that may develop occasionally under high Atlantic inflow rates from the Gibraltar strait. This regime can be also interpreted by the third EOF mode that weakens the EAG and induces a shifted anticyclone (Figures 3 and 4).

4. Discussion

[20] The available data may be used to assert a link between the two annual modes of the Alborán Sea surface circulation and the changes in the Gibraltar transport intensities. The transports through the Gibraltar Strait fluctuate at a wide range of time scales encompassing from semidiurnal, semi-annual, annual, to interannual [*Bryden et al.*, 1994; *Tsimplis and Bryden*, 2000; *García-Lafuente et al.*, 2002, 2011], except their fairly uniform values at much longer (multi-decadal) time scale [*Soto-Navarro et al.*, 2010]. Among all these fluctuations, the annual cycle is of primary importance for the present study, and primarily associated with the low frequency signals of the atmospheric pressure changes between the Atlantic and western Mediterranean and the wind stress [*Candela and Lozano*, 1994; *Bryden et al.*, 1994; *García-Lafuente et al.*, 2002; *Menemenlis et al.*, 2007]. Once these weekly to-monthly fluctuations are filtered out, the annual cycle clearly emerges on the barotropic signal indicating a relatively strong net transport in summer (which may exceed 0.5 Sv) and vice versa for winter [*Vargas-Yáñez et al.*, 2002; *García-Lafuente et al.*, 2002, 2011; *Sánchez-Román et al.*, 2009; *Soto-Navarro et al.*, 2010]. These studies further related the stronger coastal jet in summer months to the presence of a relatively weak lower layer transport such that its inertial radius is less than the curvature radius of the southeastern corner of the Strait. In such case, the inflow stops feeding the Western Anticyclonic Gyre.

[21] The implication of these observations is the presence of a relatively low range of variability for the upper layer transport over the year (say 1 ± 0.2 Sv) as compared to more noticeable winter to summer changes in the lower layer and the net transports.

[22] Based on the *García-Lafuente et al.* [2002] data set, variations in both the upper and lower layer transports near the eastern exit of Gibraltar strait predominantly confine into ± 0.3 Sv range around their mean values of 0.96 Sv and 0.83 Sv, respectively. This is confirmed by numerical studies. For instance, *Skliris and Beckers* [2009] show from numerical model a higher transport rate in summer (1.2 Sv) than in winter (1 Sv). The maximal monthly mean value is obtained during September ($\sim$1.2 Sv) in agreement with *García-Lafuente et al.* [2002] and the minimum value during February ($\sim$1.0 Sv). The transport values obtained by ORCA25 simulation in a recent study by *Vidal-Vijande et al.* [2011] are 1.076 ± 0.078 Sv of inflow (for the period 1993–2004). Flow variability displayed by the model is lower compared to the observational studies since the model data used is comprised of monthly averages and the observations contain higher frequency variability. However, given the general uncertainty, these values do enter well within the generally accepted transport values for the Strait of Gibraltar.

[23] Therefore, the single anticyclonic gyre regime may develop under moderate ranges of upper layer transport rate (1 Sv) across the Gibraltar strait whereas the double anticyclonic gyre may occur under relatively strong upper layer transport from the Gibraltar strait (>1 Sv). Below, we summarize the likely circulation regimes depending on changing Gibraltar transports.

[24] 1. In the case of extremely low upper layer transport intensity (say <1 Sv) or even its interruption due to anomalous atmospheric conditions, the AJ flows eastward along the southern coast in the form of boundary current system. This regime may have two variants; either a "purely" coastal jet mode in which the Western Anticyclonic Gyre is absent, or a "modified" coastal jet mode in which the Western Anticyclonic Gyre still continues to exist although it is not supported by the Atlantic Jet anymore. As this episode lasts not more than one-two months, a more general form should be the modified coastal jet mode that prevails prior to the disintegration of the Western Anticyclonic Gyre. Its close structural resemblance to the single anticyclonic gyre mode makes it difficult to identify by the altimeter data.

[25] 2. At moderate upper layer transport intensity ($\sim$1 Sv), the Atlantic Jet acquires one meander that circles the Western Anticyclonic Gyre and then flows in the form of coastally attached jet along the African coast. The eastern Alborán basin is covered by the cyclonic gyre Central Cyclonic Gyre. This mode occurs regularly almost every year during winter and spring months and therefore characterizes one of the quasi-persistent regimes of the circulation.

[26] 3. At relatively high upper layer transports (>1 Sv), the Atlantic Jet experiences two meanders and accompanying anticyclonic gyres (Western Anticyclonic Gyre and Eastern Anticyclonic Gyre), and the cyclonic gyre (Central Cyclonic Gyre). This system develops regularly during summer-autumn months and corresponds to the second regime of the Alborán Sea circulation. The western Algerian region to the east of the Almeria-Oran front is characterized by a permanent Eastern Cyclonic Gyre in the case of sufficiently high upper layer transport. Wavelength of the meandering AJ frontal structure may occasionally broaden and displace the Eastern Anticyclonic Gyre further east into the original position of the Eastern Cyclonic Gyre. The circulation system to the west of the Almeria-Oran front then resembles the single anticyclonic gyre circulation regime. This mode of the circulation is observed during June–October 2001 and is followed by the single anticyclonic gyre mode of the circulation. Another likely regime of higher upper layer transports is the development of three meanders of the Atlantic Jet and accompanying three anticyclonic gyres (Western Anticyclonic Gyre, Central Anticyclonic Gyre, and Eastern Anticyclonic Gyre) for duration of less than one month under favorable atmospheric conditions of autumn months. The Central Anticyclonic Gyre partially replaces the Central Cyclonic Gyre which displaces toward northern coast in the form of zonally elongated coastal eddy.

[27] Results from Table 1 suggest the years 1995, 2000 and 2006 are anomalous years since the double gyre circulation system is persistent throughout the year. As illustrated in Figure 8, the anomalous presence of the Eastern Anticyclonic Gyre and consequently the Almería Orán Front may be likely related to an intensification of the southern transport of Mediterranean waters (the so-called Northern Current (NC) [*Millot*, 1999] through the Ibiza Channel and flowing southwestward along the Spanish continental slope until Cabo de Gata (Figure 8a). Conversely, during typical years

(e.g., 2010) the retroflexion of the NC takes place north of the Ibiza Channel (Figure 8c). Therefore, the NC, advecting Mediterranean cold and more saline water may induce a sharp Almeria-Oran Front that separate them from the fresher and warmer Atlantic origin water (Figures 8b and 8d) whereas the normal years do not present such front in winter. Additionally, since these years are likely colder than a normal year (e.g., 2010, Figures 8b and 8d), a stronger winter may appear as the origin of the double gyre circulation persistence. These anomalous years are captured by the EOF analysis by the second and the third mode. They induce, at interannual timescale, an intensification of the EAG during the winter that counterbalances the non-presence of the EAG during normal years (Figures 3 and 4). As specified in section 3, although it appears a 5–6 years (Table 1 and Figure 4) periodicity for these years, the time series is too short to determinate an eventual cycle or link with synoptic variability.

[28] Finally, the temporal variability of the Alborán Sea circulation may have a direct impact on its productivity. *Macías et al.* [2009] showed that, although the Mediterranean Sea is characterized by a severe oligotrophy [*Garcia-Gorriz and Carr*, 1999], the Alborán Sea is a productive sub-basin. The different dynamic regimes described in this study control the vertical dynamics at the WAG edge as well as the horizontal advection from the shelf, which create a strip of high chlorophyll following the Atlantic Jet and the anticyclonic gyres [*Macías et al.*, 2006, 2010; *Navarro et al.*, 2011].

5. Conclusion

[29] Examination of the long-term (1993–2010) weekly Absolute Dynamic Topography and daily satellite SST data in the Alborán Sea points to two specific annually stable surface circulation regimes characterized by different meandering patterns of the Atlantic Jet and different combinations of the Western Anticyclonic Gyre, Eastern Anticyclonic Gyre and Central Cyclonic Gyre. The Western Anticyclonic Gyre exists for the entire year, but the Eastern Anticyclonic Gyre is present only during the summer-autumn period, and the location of Central Cyclonic Gyre is displaced closer to the Western Anticyclonic Gyre accordingly. Thus the annual mode is often interpreted mistakenly by the prevalence of both Western Anticyclonic Gyre and Eastern Anticyclonic Gyre for the entire year with some seasonal variations [e.g., *Pujol and Larnicol*, 2005] in contrast to those inferred by the hydrographic observations [*Viúdez et al.*, 1998; *Vargas-Yáñez et al.*, 2002; *Macías et al.*, 2008]. The annual mode of circulation is exposed to interannual variability but still remain to be robust at the decadal scale and transient changes reflect perturbations on the stable state mainly at an interannual scale. This revised interpretation makes the altimeter data analysis compatible with that of the hydrography but awaits further support in the presence of a more refined Mean Dynamic Topography field estimate and the mean SSH profile. The circulation variability may be dynamically linked to the corresponding variability of the Gibraltar transport rates.

[30] **Acknowledgments.** The altimeter products were produced by SSALTO-DUACS and distributed by AVISO with support from CNES. Partial support from EU funded projects MyOcean and PERSEUS is gratefully acknowledged. The two anonymous reviewers and Julian Kuhlmann are gratefully acknowledged for their helpful and constructive comments, which improved the quality of this study.

References

Allen, J. T., D. A. Smeed, J. Tintoré, and S. Ruiz (2001), Mesoscale subduction at the Almeria-Oran front. Part 1: Agesotrophic flow, *J. Mar. Syst.*, *30*, 263–285, doi:10.1016/S0924-7963(01)00062-8.

Bormans, M., and C. Garrett (1989), The effects of nonrectangular cross section, friction, and barotropic fluctuations on the exchange through the Strait of Gibraltar, *J. Phys. Oceanogr.*, *19*(10), 1535–1542, doi:10.1175/1520-0485(1989)019<1535:TEOROT>2.0.CO;2.

Bryden, H. L., J. Candela, and T. H. Kinder (1994), Exchange through the Strait of Gibraltar, *Prog. Oceanogr.*, *33*(3), 201–248, doi:10.1016/0079-6611(94)90028-0.

Candela, J., and C. J. Lozano (1994), Barotropic response of the western Mediterranean to observed atmospheric pressure forcing, in *The Seasonal and Interannual Variability of the Western Mediterranean Sea*, *Coastal Estuarine Stud.*, vol. 46, edited by P. La Violette, pp. 325–359, AGU, Washington, D. C.

Cazenave, A., P. Bonnefond, F. Merciera, K. Dominha, and V. Toumazou (2002), Sea level variations in the Mediterranean Sea and Black Sea from satellite altimetry and tide gauges, *Global Planet. Change*, *34*(1–2), 59–86, doi:10.1016/S0921-8181(02)00106-6.

Criado-Aldeanueva, F., F. J. Soto-Navarro, and J. García-Lafuente (2012), Seasonal and interannual variability of surface heat and freshwater fluxes in the Mediterranean Sea: Budgets and exchange through the Strait of Gibraltar, *Int. J. Climatol.*, *32*, 286–302, doi:10.1002/joc.2268.

Cusick, T. W., and M. E. Flahive (1989), *The Markov and Lagrange Spectra*, Am. Math. Soc., Providence, R. I.

Flexas, M. M., D. Gomis, S. Ruiz, A. Pascual, and P. León (2006), In situ and satellite observations of the eastward migration of the western Alborán Sea gyre, *Prog. Oceanogr.*, *70*(2–4), 486–509, doi:10.1016/j.pocean.2006.03.017.

Garcia-Gorriz, E., and M. Carr (1999), The climatological annual cycle of satellite-derived phytoplankton pigments in the Alboran Sea, *Geophys. Res. Lett.*, *26*(19), 2985–2988, doi:10.1029/1999GL900529.

García LaFuente, J., J. M. Vargas, B. Baschek, J. Candela, F. Plaza, and T. Sarhan (2000), Tides in the eastern section of the Strait of Gibraltar, *J. Geophys. Res.*, *105*(C6), 14,197–14,213, doi:10.1029/2000JC900007.

García-Lafuente, J. G., J. Delgado, J. M. Vargas, M. Vargas, F. Plaza, and T. Sarhan (2002), Low frequency variability of the exchanged flows through the Strait of Gibraltar during CANIGO, *Deep Sea Res., Part II*, *49*(19), 4051–4067, doi:10.1016/S0967-0645(02)00142-X.

García-Lafuente, J. G., A. Sánchez-Román, C. Naranjo, and J. C. Sánchez-Garrido (2011), The very first transformation of the Mediterranean outflow in the Strait of Gibraltar, *J. Geophys. Res.*, *116*, C07010, doi:10.1029/2011JC006967.

Larnicol, G., N. Ayoub, and P. Y. Le Traon (2002), Major changes in Mediterranean Sea level variability from 7 years of TOPEX/Poseidon and ERS-1/2 data, *J. Mar. Syst.*, *33–34*, 63–89, doi:10.1016/S0924-7963(02)00053-2.

Le Traon, P. Y., F. Nadal, and N. Ducet (1998), An improved mapping method of multisatellite altimeter data, *J. Atmos. Oceanic Technol.*, *15*(2), 522–534, doi:10.1175/1520-0426(1998)015<0522:AIMMOM>2.0.CO;2.

Macías, D., C. M. García, F. Echevarría, A. Vázquez, and M. Bruno (2006), Tidal induced variability of mixing processes on Camarinal Sill (Strait of Gibraltar). A pulsating event, *J. Mar. Sys*, *60*, 177–192.

Macías, D., M. Bruno, F. Echevarria, A. Vazquez, and C. M. Garcia (2008), Meteorologically induced mesoscale variability of the northwestern Alborán Sea (southern Spain) and related biological patterns, *Estuarine Coastal Shelf Sci.*, *78*, 250–266, doi:10.1016/j.ecss.2007.12.008.

Macías, D., G. Navarro, A. Bartual, F. Echevarría, and I. E. Huertas (2009), Primary production in the Strait of Gibraltar: Carbon fixation rates in relation to hydrodynamic and phytoplankton dynamics, *Estuarine Coastal Shelf Sci.*, *83*, 197–210.

Macías, D., R. Somavilla, I. González-Gordillo, and F. Echevarría (2010), Physical control of zooplankton distribution at the Strait of Gibraltar during an episode of internal wave generation, *Mar. Ecol. Prog. Ser.*, *408*, 79–95, doi:10.3354/meps08566.

Marullo, S., B. Nardelli, M. Guarracino, and R. Santoleri (2007), Observing The Mediterranean Sea from space: 21 years of Pathfinder-AVHRR sea surface temperatures (1985 to 2005): Re-analysis and validation, *Ocean Sci.*, *3*, 299–310.

Menemenlis, D., I. Fukumori, and T. Lee (2007), Atlantic to Mediterranean sea level difference driven by winds near Gibraltar Strait, *J. Phys. Oceanogr.*, *37*, 359–376, doi:10.1175/JPO3015.1.

Millot, C. (1999), Circulation in the western Mediterranean Sea, *J. Mar. Syst.*, *20*, 423–442, doi:10.1016/S0924-7963(98)00078-5.

Navarro, G., Á. Vázquez, D. Macías, M. Bruno, and J. Ruiz (2011), Understanding the patterns of biological response to physical forcing in the

Alborán Sea (western Mediterranean), *Geophys. Res. Lett.*, *38*, L23606, doi:10.1029/2011GL049708.

Parrilla, G., and T. H. Kinder (1987), Oceanografía física del mar de Alborán, *Bol. Inst. Esp. Oceanogr.*, *4*(1), 133–165.

Pascual, A., M. I. Pujol, G. Larnicol, P. Y. Le Traon, and M. H. Rio (2007), Mesoscale mapping capabilities of multisatellite altimeter missions: First results with real data in the Mediterranean Sea, *J. Mar. Syst.*, *65*, 190–211, doi:10.1016/j.jmarsys.2004.12.004.

Pujol, M. I., and G. Larnicol (2005), Mediterranean Sea eddy kinetic energy variability from 11 years of altimetric data, *J. Mar. Syst.*, *58*(3–4), 121–142, doi:10.1016/j.jmarsys.2005.07.005.

Rio, M.-H., P.-M. Poulain, A. Pascual, E. Maurib, G. Larnicol, and R. Santoleri (2007), A mean dynamic topography of the Mediterranean Sea computed from altimetric data, in-situ measurements and a general circulation model, *J. Mar. Syst.*, *65*, 484–508, doi:10.1016/j.jmarsys.2005.02.006.

Sánchez-Román, A., G. Sannino, J. García-Lafuente, A. Carillo, and F. Criado-Aldeanueva (2009), Transport estimates at the western section of the Strait of Gibraltar: A combined experimental and numerical modeling study, *J. Geophys. Res.*, *114*, C06002, doi:10.1029/2008JC005023.

Sarhan, T., J. García-Lafuente, M. Vargas, J. M. Vargas, and F. Plaza (2000), Upwelling mechanisms in the northwestern Alboran Sea, *J. Mar. Syst.*, *23*, 317–331, doi:10.1016/S0924-7963(99)00068-8.

Skliris, N., and J.-M. Beckers (2009), Modelling the Gibraltar Strait/western Alboran Sea ecohydrodynamics, *Ocean Dyn.*, *59*, 489–508, doi:10.1007/s10236-009-0185-6.

Soto-Navarro, J., F. Criado-Aldeanueva, J. García-Lafuente, and A. Sánchez-Román (2010), Estimation of the Atlantic inflow through the Strait of Gibraltar from climatological and in situ data, *J. Geophys. Res.*, *115*, C10023, doi:10.1029/2010JC006302.

Tintore, J., P. E. La Violette, I. Bladé, and A. Cruzado (1988), A study of an intense density front in the eastern Alboran Sea: The Almeria-Oran front, *J. Phys. Oceanogr.*, *18*, 1384–1397, doi:10.1175/1520-0485(1988)018<1384:ASOAID>2.0.CO;2.

Tintoré, J., D. Gomis, S. Alonso, and G. Parrilla (1991), Mesoscale dynamics and vertical motion in the Alborán Sea, *J. Phys. Oceanogr.*, *21*(6), 811–823, doi:10.1175/1520-0485(1991)021<0811:MDAVMI>2.0.CO;2.

Tsimplis, M. N., and H. L. Bryden (2000), Estimation of the transports through the Strait of Gibraltar, *Deep Sea Res., Part I*, *47*, 2219–2242, doi:10.1016/S0967-0637(00)00024-8.

Vargas-Yáñez, M., F. Plaza, J. García-Lafuente, T. Sarhan, J. M. Vargas, and P. Vélez-Belchí (2002), About the seasonal variability of the Alborán Sea circulation, *J. Mar. Syst.*, *35*, 229–248, doi:10.1016/S0924-7963(02)00128-8.

Vargas-Yáñez, M., P. Zunino, A. Benali, M. Delpy, F. Pastre, F. Moya, M. del Carmen Garcia-Martínez, and E. Tel (2010), How much is the western Mediterranean really warming and salting?, *J. Geophys. Res.*, *115*, C04001, doi:10.1029/2009JC005816.

Vélez-Belchí, P., M. Vargas-Yáñez, and J. Tintore (2005), Observation of a western Alborán gyre migration event, *Prog. Oceanogr.*, *66*, 190–210, doi:10.1016/j.pocean.2004.09.006.

Vidal-Vijande, E., A. Pascual, B. Barnier, J.-M. Molines, and J. Tintoré (2011), Analysis of a 44-year hindcast for the Mediterranean Sea: Comparison with altimetry and in situ observations, *Sci. Mar.*, *75*(1), 71–86.

Viúdez, A., J. Tintoré, and R. L. Haney (1996), Circulation in the Alborán Sea as determined by quasi-synoptic hydrographic observations. Part 1: Three-dimensional structure of the two anticyclonic gyres, *J. Phys. Oceanogr.*, *26*, 684–705, doi:10.1175/1520-0485(1996)026<0684:CITASA>2.0.CO;2.

Viúdez, A., J. M. Pinot, and R. L. Haney (1998), On the upper layer circulation in the Alborán Sea, *J. Geophys. Res.*, *103*(C10), 21,653–21,666, doi:10.1029/98JC01082.